HHS Public Access

Author manuscript

J Biomed Mater Res A. Author manuscript; available in PMC 2018 December 01.

Published in final edited form as:

J Biomed Mater Res A. 2017 December ; 105(12): 3413–3421. doi:10.1002/jbm.a.36189.

Surface Topography of Silicon Nitride Affects Antimicrobial and Osseointegrative Properties of Tibial Implants in a Murine Model

Masahiro Ishikawa[1], **Karen L. de Mesy Bentley**[1,2,3], **Bryan J. McEntire**[4], **B. Sonny Bal**[4,5], **Edward M. Schwarz**[1,2,3], and **Chao Xie**[1,3]

[1]Center for Musculoskeletal Research, University of Rochester School of Medicine and Dentistry, Rochester, NY, USA

[2]Department of Pathology & Laboratory Medicine, University of Rochester School of Medicine and Dentistry, Rochester, NY, USA

[3]Department of Orthopaedics, University of Rochester School of Medicine and Dentistry, Rochester, NY, USA

[4]Amedica Corporation, Salt Lake City, UT, USA

[5]Department of Orthopaedic Surgery, University of Missouri, Columbia, MO, USA

Abstract

While silicon nitride (Si_3N_4) is an antimicrobial and osseointegrative orthopaedic biomaterial, the contribution of surface topography to these properties is unknown. Using a methicillin-resistant strain of *Staphylococcus aureus* (MSRA), this study evaluated Si_3N_4 implants *in vitro* via scanning electron microscopy (SEM) and colony forming unit (CFU) assays, and later in an established *in vivo* murine tibia model of implant-associated osteomyelitis. *In vitro*, the "as-fired" Si_3N_4 implants displayed significant reductions in adherent bacteria versus machined Si_3N_4 (2.6×10^4 vs. 8.7×10^4 CFU, respectively; $p< 0.0002$). Moreover, SEM demonstrated that MRSA cannot directly adhere to native "as fired" Si_3N_4. Subsequently, a cross-sectional study was completed in which sterile or MRSA contaminated "as-fired" and machined Si_3N_4 implants were inserted into the tibiae of 8-week old female Balb/c mice, and harvested on day 1, 3, 5, 7, 10, or 14 post-op for SEM. The findings demonstrated that the antimicrobial activity of the "as-fired" implants resulted from macrophage clearance of the bacteria during biofilm formation on day 1, followed by osseointegration via the apparent recruitment of mesenchymal stem cells (MSC) on days 3–5, which differentiated into osteoblasts on days 7–14. In contrast, the antimicrobial behavior of the machined Si_3N_4 was due to repulsion of the bacteria, a phenomenon that also limited osteogenesis, as host cells were also unable to adhere to the machined surface. Taken together, these results suggest that the *in vivo* biological behavior of Si_3N_4 orthopaedic implants is driven by critical features of their surface nanotopography.

Corresponding author: Dr. Edward M. Schwarz, The Center for Musculoskeletal Research, University of Rochester Medical Center, 601 Elmwood Avenue, Box 665, Rochester, NY 14642, Phone: 585-275-3063, Fax: 585-275-1121, Edward_Schwarz@URMC.Rochester.edu.

Keywords

Silicon Nitride; *Staphylococcus aureus*; Antimicrobial; Osseosintegrative; Electron Microscopy

INTRODUCTION

Staphylococcus aureus is responsible for the majority of chronic osteomyelitis cases; and these bone infections remain a major challenge in orthopaedics.[1] Additionally, these infections are considered to be incurable due to biofilm dwelling bacteria that persist within *Staphylococcus* abscess communities[2, 3] (SACs, or Brodie's abscesses[4, 5]) and deep within cortical bone;[6, 7] and they cost billions of dollars each year.[8] Of particular concern is the community-associated methicillin-resistant *S. aureus* (MRSA) strain USA300LAC, which now accounts for the majority of orthopaedic infections.[9] To address this concern, silicon nitride (Si_3N_4) has emerged as an orthopaedic implant material with remarkable antimicrobial potential compared to standard clinical implants made of stainless steel (SS), poly(aryl-ether-ether-ketone) (PEEK), and titanium (Ti). In a recent time-course study, Webster *et al.* demonstrated in a Wistar rat *Staphylococcus epidermidis* infection model that new bone formation around aseptically implanted Si_3N_4 (*i.e.*, within the surgical area) was approximately 69% at 90-days post-operatively, compared with 24% and 36% for sterile PEEK and Ti implants, respectively.[10] In a parallel septic implantation arm of their study, new bone formation for Si_3N_4, Ti, and PEEK was 41%, 26%, and 21%, respectively, at this same time point. Most importantly, live bacteria were identified around PEEK (88%) and Ti (21%) implants, whereas none were present adjacent to Si_3N_4. The Si_3N_4 test samples used in the study by Webster *et al.* were identical in composition and processing to the present study. They only differed in geometry and surface finish. Furthermore, chemical, sessile-wetting, electrokinetic, microstructural, and surface roughness analyses of these same materials have been performed previously by a number of researchers.[10–14] Interested readers are referred to these earlier studies for comparative details.

Another critical biomaterial property of orthopaedic implants is their compatibility within the bone microenvironment to allow for mesenchymal stem cell (MSC) adherence, differentiation, activation of bone forming osteoblasts, and overall osseointegration into the host bone.[11] In this regard, Si_3N_4 implants have also been shown to have remarkable advantages for orthopaedic applications, as quantitative assessment of osseointegration measured by resistance to implant push-out at 3-months post-implantation in a rat model demonstrated statistically superior bone growth and attachment compared with Ti and PEEK.[10] However, while empirical antimicrobial and osseosintegrative biomaterial properties of Si_3N_4 implants have been established,[12] the contribution of surface topography to these properties remains unknown. Therefore, this study was designed to evaluate *S. aureus* biofilm formation on two forms of Si_3N_4 standard implants ("as-fired" and machined), versus SS, Ti, and PEEK implants *in vitro.* Thus, we performed descriptive scanning electron microscopy (SEM) studies of the behaviors of MRSA, macrophages, MSCs, and osteoblasts on the surface of "as-fired" versus machined Si_3N_4 implants in an established murine model of implant-associated osteomyelitis,[15] to test the hypothesis that

surface topography of Si_3N_4 implants contributes to their antimicrobial and osseosintegrative properties *in vitro* and *in vivo*.

MATERIALS AND METHODS

L-shaped murine implant fabrication

Flat wire (cross-section 0.2 mm × 0.5 mm; MicroDyne Technologies, Plainville, CT) was used to generate L-shaped SS and Ti implants as previously described.[15] Briefly, the wire was cut to 4 mm length, and bent into an L-shaped implant: long side 3 mm, short side 1 mm. Similarly L-shaped PEEK and Si_3N_4 implants were fabricated by Amedica Corporation (Salt Lake City, UT). PEEK stock (PEEK Optima®, ASTM F2026-16, Invibio®, West Conshohocken, PA) was machined into the L-shaped specimens using computer numerical controlled (CNC) machining equipment (Haas Office Mill, Haas Automation, Oxnard, CA). Two groups of Si_3N_4 L-shaped specimens were also produced via conventional ceramic fabrication techniques. They differed only in their surface morphology and final heat-treatment. Both groups were prepared by mixing and spray-drying Si_3N_4 powder (Ube SN-E10, Ube City, Japan), yttrium oxide (Y_2O_3, Grade C, H. C. Starck, Munich, Germany) and aluminum oxide (Al_2O_3, SA8-DBM, Baikowski/Malakoff, Charlotte, NC) at percentages of 90.0, 6.0, and 4,0 wt%., respectively, along with appropriate binders and pressing aids. The resulting powder was pressed into rectangular blocks via uniaxial compacting equipment (TPA 30, Dorst America, Bethlehem, PA) at pressures in excess of 200 MPa. The specimens' features were then machined (Haas Office Mill) in their pressed state to shrink to either final- or near-final-size during subsequent densification heat-treatments. Samples were fired at a temperature in excess of 1700°C in a N_2 environment (CVI Belt and Batch Furnaces, Centorr-Vacuum Industries, Nashua, NH) to obtain closed-porosity, and further densified using hot-isostatic pressing (QIH 21, Avure Autoclave Systems, Columbus, OH) at a temperature exceeding 1650°C and N_2 gas pressures of >200 MPa. After densification, one group required no further processing and was designated "as-fired". The morphology of this group of samples consisted of fine nano- to micron-size anisotropic prismatic ß-Si_3N_4 grains which projected from the surface of each specimen (Fig. 1(A)). The second group of Si_3N_4 specimens was ground flat using a 120 grit diamond wheel on a surface grinder (Okamoto 12-24D Grind-X, Vernon Hills IL). The surface grinding operation removed the protruding grains from the surface, leaving only ground features (Fig. 1(B)). After grinding, these samples were subjected to a N_2-annealing heat-treatment at 1400°C for 30 minutes.

MRSA inoculation of implants

Static cultures of a methicillin-resistant strain of *Staphylococcus aureus* (USA300 LAC)[16] were obtained via overnight culture (O.D. = 0.7 at 630nm) of the bacteria in 10ml of tryptic soy broth (TSB) media at 37°C,[17] which was used to contaminate the L-shaped implants (n=4) as previously described.[15] Based on established protocols known to contaminate SS pins with 10^5 CFU of planktonic *S. aureus*,[15, 18] implants were incubated in the MRSA culture for 20 minutes at room temperature, and then air dried for 5 minutes. To determine the inoculum, implants were placed into Eppendorf tubes with 1 ml of sterile saline, vortexed for 2 minutes, and 10-fold dilutions were plated on TSA to quantify CFUs after 24 hr incubation at 37°C. To assess differences between numbers of adherent MRSA on SS, Ti,

PEEK, and Si_3N_4 ("as-fired" and machined) surfaces following *in vitro* exposure, two independent experiments with the five different implants (n=4) were assess via CFU assay.

Statistical Analysis

The results from the *in vitro* CFU assay studies were assess to determine significant differences versus "as-fired" Si_3N_4. The mean +/− standard deviation (SD) CFU from each group (n=4) was determined, and significant differences were determined via 1-way ANOVA in which $p<0.05$ was considered significant.

Scanning Electron Microscopy (SEM)

SEM was performed a previously described.[15] Briefly, the implants from the *in vitro* studies were placed into 24 well plates, fixed in 2.5% glutaraldehyde/4% paraformaldehyde in 0.1M cacodylate overnight and post-fixed in buffered 1% osmium tetroxide. A pipet tip was placed against the wall of the wells, for fluid exchange or removal to reduce disruption of biofilm during dehydration in a graded series of ethanol to 100%. The pins were then critically point dried, mounted onto aluminum stubs and sputtercoated with gold prior to imaging using a Zeiss Auriga FE SEM. Three SEM micrographs per sample group were randomly chosen for descriptive analysis.

In vivo studies

All *in vivo* experiments were performed following protocols approved by the University of Rochester Committee on Animal Resources. After sterilization and incubation in sterile saline or an overnight culture of USA300 LAC, the air-dried L-shaped implants were surgically introduced into 8-week-old female Balb/c mice (Jackson Lab, Bar Harbor, ME). The surgical approach to press-fit the L-shaped trans-tibial implants from the medial to the lateral side was performed as previously described.[15] For cross-sectional *ex vivo* implant surface analysis, mice (n=3) were euthanized on day 1, 3, 5, 7, 10, or 14. The tibiae were surgically removed with the implant intact, and fixed in 2.5% glutaraldehyde and 4% paraformaldehyde in 0.1M sodium cacodylate buffer overnight then decalcified in 14% EDTA for 3 to 4 days, to facilitate removal of the implant and reduce the risk of damage to the biofilm. An incision into the bone facilitated the lifting out (perpendicular to the tibia) so any soft tissue adhering to the topside (the side to be evaluated by SEM) of the implant was retained intact. The implants were transferred to 24 well plates into PBS for SEM processing as described above.

RESULTS

Differential responses of "as-fired" versus machined Si_3N_4 implants to MRSA exposure in vitro

To directly evaluate the antimicrobial surfaces of Si_3N_4 implants versus SS, Ti, and PEEK, SEM analyses were immediately conducted on the implants after *in vitro* exposure to MRSA. The results showed that large numbers of bacteria adhered to Ti and PEEK, with fewer numbers on SS and machined Si_3N_4 implants (Figs. 2(A-J)). Remarkably, no bacteria were observed on native "as fired" Si_3N_4 implant surfaces (Fig. 2(I)). However, a closer inspection of the Si_3N_4 implants revealed bacteria bound to foreign material and culture

debris on “as fired” surfaces (Figs. 2(K-N)), and preferential bacterial adhesion to the flatter surfaces of the incompletely machined implants (Figs. 2(O-R)). Collectively, these findings suggest that MRSA cannot directly adhere to native “as fired” Si_3N_4 implant surfaces despite the opportunities afforded by the expanded surface area and crevices for 1 μm diameter cocci to reside in. Moreover, these antimicrobial properties are largely due to surface topography, as they are lost by machining the surface.

To validate the descriptive SEM findings, CFUs on the surface of the implants were quantified following *in vitro* exposure to the overnight culture of MRSA (Figure 3). The results demonstrated a significant 1.78, 4.43, and 2.84-fold reduction in CFU on “as-fired” Si_3N_4 implants versus SS, Ti, and PEEK respectively ($p<0.001$). Additionally, similar numbers of CFUs were recovered from machined Si_3N_4 versus SS, Ti, and PEEK implants, while a significant 3.3-fold reduction in CFU on “as-fired” versus machined Si_3N_4 implants was observed ($p=0.0019$). Taken together, these *in vitro* exposure findings demonstrate the critical importance of surface topography for the inherent antimicrobial properties of “as-fired” Si_3N_4 implants, as MRSA cannot adhere directly to its native surface, but can adhere with similar affinity as it does on SS, Ti, and PEEK implants when its native surface is machined and nitrogen annealed.

Differential host responses to sterile and septic “as-fired” vs. machined Si_3N_4 implants in vivo

To assess the effects of surface topography on Si_3N_4 implants *in vivo*, an established murine tibia model was utilized.[15] Initially, a cross-sectional time course evaluation was performed using sterile “as-fired” versus machined Si_3N_4 implants harvested from mice on days 1, 3, 5, 7, 10, and 14 after tibial insertion, via descriptive SEM (Figure 4). The results demonstrated that the highly reactive “as fired” Si_3N_4 implant surface progressively transformed towards osseointegration over time as follows. Phenotypically, “as fired” Si_3N_4 implant surfaces were highly reactive with host factors and blood cells shortly after implantation, as evidenced by the rich fibrin coating and presence of leukocytes and erythrocytes attached to this matrix (Figs. 4B, B^1). By day 3, rounded/oval cells morphologically consistent with mesenchymal stem cells (MSCs) were present on the surface (Figs. 4D, D^1). The prominent cells on the implant surface on day 5 were rounded to polygonal in appearance, and were phenotypically consistent with differentiating MSCs (Figs. 4F, F^1). Large polygonal mesenchymal cells consistent with an osteoblast phenotype first appeared on “as fired” Si_3N_4 implant surfaces on day 7 (Figs. 4N, N^1), and thereafter these implants were primarily occupied by osteoblastic cells organizing to form a dense coating (Figs. 4P, P^1, R, R^1). In contrast, machined Si_3N_4 implant surfaces were largely non-reactive with the host, and did not display any remarkable changes over time (Figs. 4G-L, S-X).

To assess the effects of surface topography on septic Si_3N_4 implants *in vivo*, the descriptive SEM cross-sectional time course study was repeated for “as fired” versus machined Si_3N_4 implants that were exposed to a MRSA overnight culture prior to surgical implantation (Figure 5). These results also showed that the highly reactive “as fired” Si_3N_4 implant surface displayed a progressive transformation from a MRSA infected condition to an apparent pre-osseous interface over time. On day 1 post-op, bacterial biofilm on the implant

surface appeared to be attacked by inflammatory cells (Fig. 5B), and the mature bacterial biofilm pods appeared elevated from the surface by inflammatory cells anchored with fibrin cables on day 3 (Fig. 5D). On day 5, the eradicated bacteria appeared to be replaced by a mixture of round cells, which were morphologically consistent with macrophages, together with small numbers of polygonal cells (Fig. 5F). Thereafter, the "as fired" Si_3N_4 implant surface was covered with polarized cells with an osteoblastic appearance (Figs. 5G-H). In contrast, machined Si_3N_4 implant surfaces were less reactive with both bacteria and host cells. Bacteria were rarely found in biofilms on implants harvested 1-day post-op (Fig. 5N). By day 3, no bacteria were found, and few activated macrophages were appeared on the surface (Fig. 5P). Thereafter, machined Si_3N_4 implant surfaces were incompletely coated by red and white blood cells (Figs. 5Q-X).

DISCUSSION

Bone infections are the bane of orthopaedic surgery, of which the vast majority are caused by *Staphylococcal* species.[1] While the number of bone infections following primary elective surgery is low (1–5%), reinfection rates are very high (15–40%),[19–23] which has led to the orthopaedic paradigm that *S. aureus* infection of bone is incurable.[24] Additionally, surgical site infections are known to be a non-random event that is largely determined by patient-specific factors, as infections are caused by only a few prevalent nosocomial strains (*i.e.* MRSA USA300);[25] and implementation of the most rigorous surgical systems (*i.e.* Surgical Care Improvement Project (SCIP) measures) is incapable of reducing infection rates below 1%.[26, 27] Moreover, ~13% of orthopaedic patients infected with *S. aureus* become septic and die from multiorgan failure.[28–30] Thus, there has been a tremendous quest to produce antimicrobial implants. In general, these efforts have been largely focused on coating existing orthopaedic implants with: 1) metal ions (*e.g.* silver[31] and copper[32]) which has proven to be limited due to toxicity issues;[33] and 2) antibiotics (*e.g.* gentamicin[34] and vancomycin[35]) which limits the osteoconduction of the implant. Thus, an important alternative approach is to find an implantable biomaterial that is inherently antimicrobial and osteoconductive.

Si_3N_4 is a synthetic non-oxide ceramic that is used in many industrial applications, and has been investigated or adapted as a biomedical material since 1989.[10, 12, 36–42] The rationale for using Si_3N_4-based implants in skeletal reconstruction is based on its favorable combination of mechanical strength, microstructure, and cytotoxicity.[12, 41] Polished and porous implants made of Si_3N_4 have shown encouraging outcomes in spine and maxillofacial surgery.[12, 41] Most interestingly, initial studies have demonstrated that Si_3N_4 is empirically antimicrobial and osteoconductive,[10] making it a very attractive biomaterial for orthopaedic surgery. In contrast to the limited clinical experience with Si_3N_4, implants made of SS, Ti, and their alloys have been used in skeletal reconstruction for many decades.[43, 44] More recently, PEEK, a polymer with modest strength and a low modulus of elasticity compared with metal, has been investigated as an orthopedic biomaterial,[45] and is commonly used in spine surgery.[46] However, SS, Ti, and PEEK are not known to have inherent antimicrobial activities. Thus, this head-to-head study assessed the ability of MRSA to adhere to SS, Ti, PEEK, and Si_3N_4 implants *in vitro*. Additionally, as the role of surface topography in bacterial adherence to Si_3N_4 implants is unknown, "as fired" versus machined

Si_3N_4 implants were also compared. While the results of these *in vitro* experiments with MRSA (Figs. 2 and 3) corroborated prior studies demonstrating greater antimicrobial effects of Si_3N_4 implants compared to SS, Ti, and PEEK,[10,12] the more interesting observation was that MRSA cannot directly bind to the "as fired" Si_3N_4 implant surface (Figs. 2(I), 2(K)–2(N)). However, removal of the nanotopography via machining and nitrogen annealing rendered Si_3N_4 implants susceptible to MRSA adhesion (Figs. 2(J), 2(O)–2(R)). It was also interesting to find that SS implants displayed greater antimicrobial activity versus Ti implants, as assessed in our *in vitro* CFU assay (Fig. 3). As this finding is somewhat inconsistent with prior studies that have failed to observe similar findings,[47–49] follow up experiments are warranted. While the present study did not delve into the mechanisms responsible for the observed differences, the enhanced resistance to MRSA by the "as-fired" Si_3N_4 may be two-fold. First, the acicular pillared nanostructured features of the "as-fired" surface inhibited initial attachment of MRSA cells. Secondly, there may be a chemical resistance associated with the minute elution of an oxidative form of nitrogen (*i.e.*, peroxynitrite, $ONOO^-$). These combined mechanisms are plausible based on research from other investigators. For instance, Xu *et al.* demonstrated that a combination of nano-pillared polyurethane biomaterial (400 to 500 nm spikes) doped with a nitrogen emitting compound (S-nitroso-N-acetylpenicillamine) was more effective in inhibiting the bacterial adhesion of *Staphylococcus epidermidis* than either treatment method alone;[50] and Pezzotti *et al.* specifically showed that the release of nitrogen from Si_3N_4 in the form of peroxynitrite was an effective deterrent in the attachment of *Porphyromonas gingivalis*.[51] Undoubtedly, the topography and higher surface area associated with "as-fired" in comparison to "machined" Si_3N_4 enhanced both mechanistic effects.

In order to best assess *in vivo* responses to "as fired" and machined Si_3N_4 implants within the bone microenvironment, a murine tibia model designed to quantify biofilm formation within a prospective $1mm^2$ region of interest (ROI) was chosen.[15] It was surprising to discover that the murine host response to these Si_3N_4 implants was Boolean, as the vast majority of the "as fired" surface was covered by day 1 post-op, while the machined surface remained naked throughout the 14 day study period (Figure 4). Similarly, the analyzed ROIs of MRSA contaminated Si_3N_4 implants showed that the "as fired" surfaces were dramatically more reactive with the host, rendering quantitative assessment of differences in the % surface coverage meaningless. Thus, while a notable weakness of these *in vivo* studies is the absence of quantitative analyses, the primary goal of identifying important differences between "as fired" and machined Si_3N_4 surfaces was achieved. Moreover, the study provided important insights into the antimicrobial and osteoconductive mechanisms of this unique biomaterial. Specifically, several hypothesis were generated on observations that will serve as the scientific premise of future studies, including: 1) the inability of MRSA to directly adhere to native "as fired" surfaces (Figs. 5B, D); 2) the ability of host inflammatory cells and extracellular matrix fibers to elevate MRSA biofilm/pods from the "as fired" surface to allow effective bacterial clearance by phagocytes (Figs. 5A-F); and 3) the transformation from an inflammatory cell coated surface (Fig. 5F) to an osteoblastic coated surface (Figs. 5E-L). On the negative side, observations demonstrating minimal host cell interactions with machined and nitrogen-annealed Si_3N_4 surfaces diminish enthusiasm for future studies with these types of implants.

In addition to the absence of quantitative outcome measures, there are three other notable limitations of this study. The first is that only USA300 was evaluated, rather than a multitude of methicillin sensitive and resistant strains of *S. aureus* that represent clinical infections. The decision to focus this exploratory study on USA300 was based on publications indicating that this MRSA strain is the most prevalent in surgical site infections,[9, 25] and that different *S. aureus* strains behave similarly in the murine implant model.[15] It is also known that the presence of human serum/plasma can impact bacterial adhesion to implant surfaces.[52] Thus, appropriate follow-up studies are need to confirm the clinical significance of our findings. The other limitation is the absence of formal radiographic, biomechanical, and histological analyses to assess osseointegration of "as fired" versus machined Si_3N_4 implants. As these are critical factors that will determine the clinical utility of Si_3N_4 implants for various indications, future studies to established differences and elucidate their osteoconductive mechanisms are warranted.

Acknowledgments

The authors wish to thank Gayle Schneider of the URMC Electron Microscope Shared Resource Laboratory for her technical assistance.

Conflicts of interest: Bryan J. McEntire, MBA, PhD, is Chief Technology Officer of Amedica Corporation. He has received stock and is a paid employee.

B. Sonny Bal, MD, JD, MBA, is Chairman of the Board, Chief Executive Officer, President and Principal Financial Officer of Amedica Corporation. He has received stock and financial compensation.

Grant sponsors: Amedica Corporation and National Institutes of Health, Grant number: P30 AR069655, P50 AR072000.

References

1. Darouiche RO. Treatment of infections associated with surgical implants. N Engl J Med. 2004 Apr 1; 350(14):1422–9. [PubMed: 15070792]
2. Cheng AG, Kim HK, Burts ML, Krausz T, Schneewind O, Missiakas DM. Genetic requirements for Staphylococcus aureus abscess formation and persistence in host tissues. FASEB J. 2009 Oct; 23(10):3393–404. [PubMed: 19525403]
3. Cheng AG, McAdow M, Kim HK, Bae T, Missiakas DM, Schneewind O. Contribution of coagulases towards Staphylococcus aureus disease and protective immunity. PLoS Pathog. 2010 Aug 05.6(8):e1001036. [PubMed: 20700445]
4. Brodie BC. Pathological Researches respecting the Diseases of Joints. Med Chir Trans. 1813; 4:210–80.
5. Brodie BC. An Account of some Cases of Chronic Abscess of the Tibia. Med Chir Trans. 1832; 17:239–49.
6. Brady RA, Leid JG, Calhoun JH, Costerton JW, Shirtliff ME. Osteomyelitis and the role of biofilms in chronic infection. FEMS Immunol Med Microbiol. 2008 Jan; 52(1):13–22. Epub 2007/12/18. [PubMed: 18081847]
7. de Mesy Bentley KL, Trombetta R, Nishitani K, Bello-Irizarry SN, Ninomiya M, Zhang L, et al. Evidence of Staphylococcus aureus Deformation, Proliferation and Migration in Canaliculi of Live Cortical Bone in Murine Models of Osteomyelitis. J Bone Miner Res. 2016 Dec 08. In Press.
8. Hernandez-Vaquero D, Fernandez-Fairen M, Torres A, Menzie AM, Fernandez-Carreira JM, Murcia-Mazon A, et al. Treatment of periprosthetic infections: an economic analysis. ScientificWorldJournal. 2013; 2013:821650. [PubMed: 23781163]
9. Kourbatova EV, Halvosa JS, King MD, Ray SM, White N, Blumberg HM. Emergence of community-associated methicillin-resistant Staphylococcus aureus USA 300 clone as a cause of

health care-associated infections among patients with prosthetic joint infections. Am J Infect Control. 2005 Sep; 33(7):385–91. Epub 2005/09/13. [PubMed: 16153484]

10. Webster TJ, Patel AA, Rahaman MN, Sonny Bal B. Anti-infective and osteointegration properties of silicon nitride, poly(ether ether ketone), and titanium implants. Acta Biomater. 2012 Dec; 8(12): 4447–54. Epub 2012/08/07. [PubMed: 22863905]
11. Lewallen EA, Riester SM, Bonin CA, Kremers HM, Dudakovic A, Kakar S, et al. Biological strategies for improved osseointegration and osteoinduction of porous metal orthopedic implants. Tissue Eng Part B Rev. 2015 Apr; 21(2):218–30. [PubMed: 25348836]
12. Bal BS, Rahaman MN. Orthopedic applications of silicon nitride ceramics. Acta Biomater. 2012 Aug; 8(8):2889–98. [PubMed: 22542731]
13. Bock RM, McEntire BJ, Bal BS, Rahaman MN, Boffelli M, Pezzotti G. Surface modulation of silicon nitride ceramics for orthopaedic applications. Acta Biomater. 2015 Oct.26:318–30. Epub 2015/08/26. [PubMed: 26302831]
14. Bock RM, Jones EN, Ray DA, Sonny Bal B, Pezzotti G, McEntire BJ. Bacteriostatic behavior of surface modulated silicon nitride in comparison to polyetheretherketone and titanium. J Biomed Mater Res A. 2017 May; 105(5):1521–34. Epub 2016/12/22. [PubMed: 28000413]
15. Nishitani K, Sutipornpalangkul W, de Mesy Bentley KL, Varrone JJ, Bello-Irizarry SN, Ito H, et al. Quantifying the natural history of biofilm formation in vivo during the establishment of chronic implant-associated Staphylococcus aureus osteomyelitis in mice to identify critical pathogen and host factors. J Orthop Res. 2015 Sep; 33(9):1311–9. [PubMed: 25820925]
16. Guo Y, Ramos RI, Cho JS, Donegan NP, Cheung AL, Miller LS. In vivo bioluminescence imaging to evaluate systemic and topical antibiotics against community-acquired methicillin-resistant Staphylococcus aureus-infected skin wounds in mice. Antimicrob Agents Chemother. 2013 Feb; 57(2):855–63. [PubMed: 23208713]
17. Varrone JJ, de Mesy-Bentley KL, Nishitani K, Hunter JG, Kates SL, Daiss JL, et al. Passive Immunization with Anti-Glucosaminidase Monoclonal Antibodies Protects Mice from Implant-Associated Osteomyelitis, Inhibits Biofilm formation, and Mediates Opsonophagocytosis of Staphylococcus aureus Megaclusters. J Ortho Res. 2013 Submitted.
18. Li D, Gromov K, Soballe K, Puzas JE, O'Keefe RJ, Awad H, et al. Quantitative mouse model of implant-associated osteomyelitis and the kinetics of microbial growth, osteolysis, and humoral immunity. J Orthop Res. 2008 Jan; 26(1):96–105. [PubMed: 17676625]
19. Azzam K, McHale K, Austin M, Purtill JJ, Parvizi J. Outcome of a second two-stage reimplantation for periprosthetic knee infection. Clin Orthop Relat Res. 2009 Jul; 467(7):1706–14. Epub 2009/02/19. [PubMed: 19224302]
20. Ghanem E, Azzam K, Seeley M, Joshi A, Parvizi J. Staged revision for knee arthroplasty infection: what is the role of serologic tests before reimplantation? Clin Orthop Relat Res. 2009 Jul; 467(7): 1699–705. Epub 2009/02/26. [PubMed: 19241115]
21. Parvizi J, Azzam K, Ghanem E, Austin MS, Rothman RH. Periprosthetic infection due to resistant staphylococci: serious problems on the horizon. Clin Orthop Relat Res. 2009 Jul; 467(7):1732–9. Epub 2009/05/02. [PubMed: 19408061]
22. Ferry T, Uckay I, Vaudaux P, Francois P, Schrenzel J, Harbarth S, et al. Risk factors for treatment failure in orthopedic device-related methicillin-resistant Staphylococcus aureus infection. Eur J Clin Microbiol Infect Dis. 2009 Feb; 29(2):171–80. Epub 2009/12/01. [PubMed: 19946789]
23. Salgado CD, Dash S, Cantey JR, Marculescu CE. Higher risk of failure of methicillin-resistant Staphylococcus aureus prosthetic joint infections. Clin Orthop Relat Res. 2007 Aug.461:48–53. Epub 2007/05/31. [PubMed: 17534195]
24. Schwarz EM, Alt V, Kates SL. The 1st international consensus meeting on periprosthetic joint infection. J Orthop Res. 2014 Jan.32(Suppl 1):S1. [PubMed: 24464881]
25. Limbago B, Fosheim GE, Schoonover V, Crane CE, Nadle J, Petit S, et al. Characterization of methicillin-resistant Staphylococcus aureus isolates collected in 2005 and 2006 from patients with invasive disease: a population-based analysis. J Clin Microbiol. 2009 May; 47(5):1344–51. Epub 2009/03/27. [PubMed: 19321725]
26. Auerbach A. Healthcare quality measurement in orthopaedic surgery: current state of the art. Clin Orthop Relat Res. 2009 Oct; 467(10):2542–7. [PubMed: 19381743]

27. Aslam S, Darouiche RO. Prosthetic joint infections. Curr Infect Dis Rep. 2012 Oct; 14(5):551–7. [PubMed: 22847032]
28. van Hal SJ, Jensen SO, Vaska VL, Espedido BA, Paterson DL, Gosbell IB. Predictors of mortality in Staphylococcus aureus Bacteremia. Clin Microbiol Rev. 2012 Apr; 25(2):362–86. [PubMed: 22491776]
29. Cram P, Lu X, Kates SL, Singh JA, Li Y, Wolf BR. Total knee arthroplasty volume, utilization, and outcomes among Medicare beneficiaries, 1991–2010. JAMA. 2012 Sep 26; 308(12):1227–36. Epub 2012/09/27. [PubMed: 23011713]
30. Gedbjerg N, Larosa R, Hunter JG, Varrone JJ, Kates SL, Schwarz EM, et al. Anti-Glucosaminidase IgG in Sera as a Biomarker of Host Immunity Against Staphylococcus aureus in Orthopaedic Surgery Patients. J Bone Joint Surg Am. 2013 Nov 20; 95(22):e1711–9.
31. Gosheger G, Hardes J, Ahrens H, Streitburger A, Buerger H, Erren M, et al. Silver-coated megaendoprostheses in a rabbit model–an analysis of the infection rate and toxicological side effects. Biomaterials. 2004 Nov; 25(24):5547–56. [PubMed: 15142737]
32. Hoene A, Prinz C, Walschus U, Lucke S, Patrzyk M, Wilhelm L, et al. In vivo evaluation of copper release and acute local tissue reactions after implantation of copper-coated titanium implants in rats. Biomed Mater. 2013 Jun.8(3):035009. [PubMed: 23598370]
33. Sansone V, Pagani D, Melato M. The effects on bone cells of metal ions released from orthopaedic implants. A review. Clin Cases Miner Bone Metab. 2013 Jan; 10(1):34–40. [PubMed: 23858309]
34. Alt V, Bitschnau A, Osterling J, Sewing A, Meyer C, Kraus R, et al. The effects of combined gentamicin-hydroxyapatite coating for cementless joint prostheses on the reduction of infection rates in a rabbit infection prophylaxis model. Biomaterials. 2006 Sep; 27(26):4627–34. Epub 2006/05/23. [PubMed: 16712926]
35. Antoci V Jr, King SB, Jose B, Parvizi J, Zeiger AR, Wickstrom E, et al. Vancomycin covalently bonded to titanium alloy prevents bacterial colonization. J Orthop Res. 2007 Jul; 25(7):858–66. Epub 2007/04/07. [PubMed: 17415753]
36. Howlett CR, McCartney E, Ching W. The effect of silicon nitride ceramic on rabbit skeletal cells and tissue. An in vitro and in vivo investigation. Clin Orthop Relat Res. 1989 Jul.(244):293–304.
37. Kue R, Sohrabi A, Nagle D, Frondoza C, Hungerford D. Enhanced proliferation and osteocalcin production by human osteoblast-like MG63 cells on silicon nitride ceramic discs. Biomaterials. 1999 Jul; 20(13):1195–201. [PubMed: 10395388]
38. Amaral M, Costa MA, Lopes MA, Silva RF, Santos JD, Fernandes MH. Si(3)N(4)-bioglass composites stimulate the proliferation of MG63 osteoblast-like cells and support the osteogenic differentiation of human bone marrow cells. Biomaterials. 2002 Dec; 23(24):4897–906. [PubMed: 12361631]
39. Amaral M, Lopes MA, Santos JD, Silva RF. Wettability and surface charge of Si3N4-bioglass composites in contact with simulated physiological liquids. Biomaterials. 2002 Oct; 23(20):4123–9. [PubMed: 12182314]
40. Amaral M, Lopes MA, Silva RF, Santos JD. Densification route and mechanical properties of Si3N4-bioglass biocomposites. Biomaterials. 2002 Feb; 23(3):857–62. [PubMed: 11771704]
41. Neumann A, Unkel C, Werry C, Herborn CU, Maier HR, Ragoss C, et al. Prototype of a silicon nitride ceramic-based miniplate osteofixation system for the midface. Otolaryngol Head Neck Surg. 2006 Jun; 134(6):923–30. [PubMed: 16730531]
42. Guedes e Silva CC, Konig B Jr, Carbonari MJ, Yoshimoto M, Allegrini S Jr, Bressiani JC. Tissue response around silicon nitride implants in rabbits. J Biomed Mater Res A. 2008 Feb; 84(2):337–43. [PubMed: 17607762]
43. Dabrowski B, Swieszkowski W, Godlinski D, Kurzydlowski KJ. Highly porous titanium scaffolds for orthopaedic applications. J Biomed Mater Res B Appl Biomater. 2010 Oct; 95(1):53–61. [PubMed: 20690174]
44. Pohler OE. Unalloyed titanium for implants in bone surgery. Injury. 2000 Dec; 31(Suppl 4):7–13.
45. Kurtz SM, Devine JN. PEEK biomaterials in trauma, orthopedic, and spinal implants. Biomaterials. 2007 Nov; 28(32):4845–69. [PubMed: 17686513]
46. Toth JM, Wang M, Estes BT, Scifert JL, Seim HB 3rd, Turner AS. Polyetheretherketone as a biomaterial for spinal applications. Biomaterials. 2006 Jan; 27(3):324–34. [PubMed: 16115677]

47. Rochford ET, Richards RG, Moriarty TF. Influence of material on the development of device-associated infections. Clin Microbiol Infect. 2012 Dec; 18(12):1162–7. Epub 2012/08/29. [PubMed: 22925523]

48. Ribeiro M, Monteiro FJ, Ferraz MP. Infection of orthopedic implants with emphasis on bacterial adhesion process and techniques used in studying bacterial-material interactions. Biomatter. 2012 Oct-Dec;2(4):176–94. Epub 2013/03/20. [PubMed: 23507884]

49. Arens S, Schlegel U, Printzen G, Ziegler WJ, Perren SM, Hansis M. Influence of materials for fixation implants on local infection. An experimental study of steel versus titanium DCP in rabbits. J Bone Joint Surg Br. 1996 Jul; 78(4):647–51. Epub 1996/07/01. [PubMed: 8682836]

50. Xu LC, Wo Y, Meyerhoff ME, Siedlecki CA. Inhibition of bacterial adhesion and biofilm formation by dual functional textured and nitric oxide releasing surfaces. Acta Biomater. 2017 Mar 15.51:53–65. Epub 2017/01/15. [PubMed: 28087484]

51. Pezzotti G, Bock RM, McEntire BJ, Jones E, Boffelli M, Zhu W, et al. Silicon Nitride Bioceramics Induce Chemically Driven Lysis in Porphyromonas gingivalis. Langmuir. 2016 Mar 29; 32(12): 3024–35. Epub 2016/03/08. [PubMed: 26948186]

52. Daeschel MA, McGuire J. Interrelationships between protein surface adsorption and bacterial adhesion. Biotechnol Genet Eng Rev. 1998; 15:413–38. Epub 1998/05/09. [PubMed: 9573612]

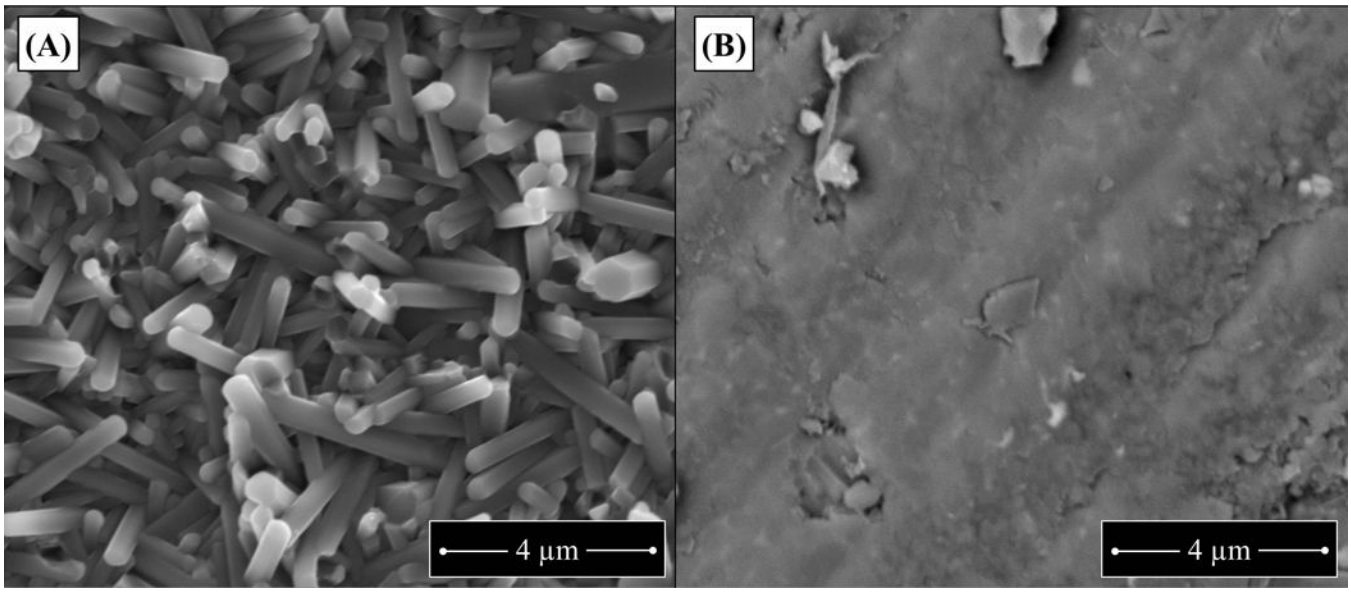

Figure 1. Topographical differences of native "as fired" and machined Si_3N_4 implant surfaces

Si_3N_4 "as fired" and machined implants were fabricated and directly imaged by SEM as described in methods. Representative SEM images of these starting materials are shown to illustrate the fine nano- to micron-size anisotropic prismatic ß-Si_3N_4 grains projecting from the "as fired" surface (A), versus the smooth annealed surface of machined Si_3N_4 (B).

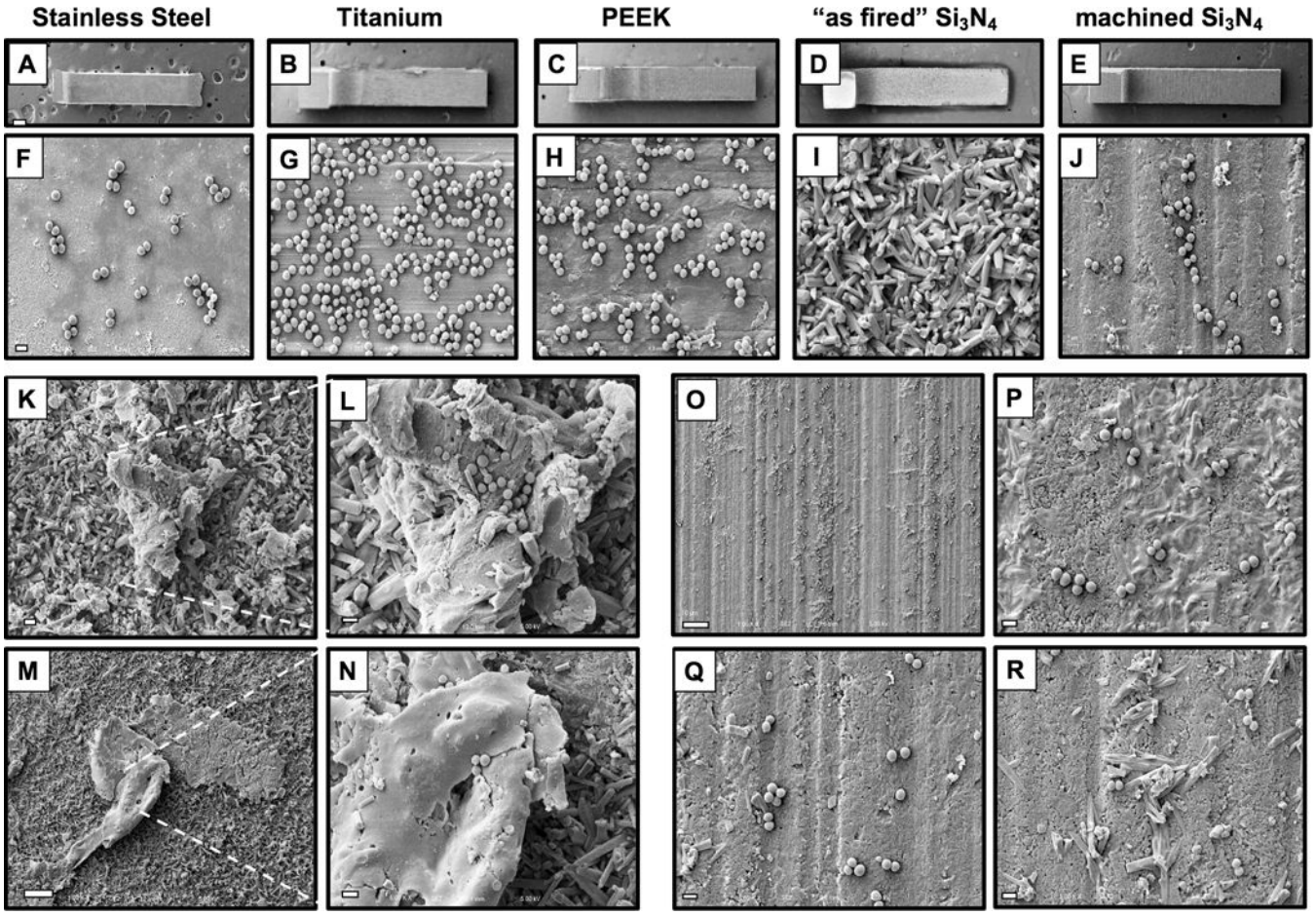

Figure 2. Native "as fired" Si_3N_4 implant surfaces are highly resistant to MRSA adherence in vitro

SS, Ti, PEEK, "as fired" Si_3N_4 and machined Si_3N_4 implants (n=4) were submerged in an overnight culture (O.D. = 0.7 at 630nm) of USA300LAC, air dried, and processed for SEM. Representative low power images of the L-shaped implants are shown at ×30 (A-E; scale bar in A = 200μm), and higher power images of regions containing adherent MSRA are shown at ×5,000 (F-J; scale bar in F = 1μm). Of note is that we failed to identify bacteria that were directly adhering to native "as fired" Si_3N_4 implant surfaces (I). However, bacteria were only observed on foreign material and culture debris (TSB precipitate and lysed bacteria) that adhered to the "as fired" Si_3N_4 implant surfaces (K ×2,000; scale bar = 5μm; inset image (L) ×5,000 scale bar = 1μm) and (M ×1,000 ; scale bar = 10μm; inset image (N) ×5,000 scale bar = 1μm). In contrast, bacteria were readily found on machined Si_3N_4 implant surfaces (O ×1,000 scale bar = 10μm). High power images of non-uniformly machined areas demonstrated preferential bacterial adhesion to the flatter surfaces, and lack of bacterial adhesion to incompletely machined surface structures (P-R ×5,000 scale bar = 1μm).

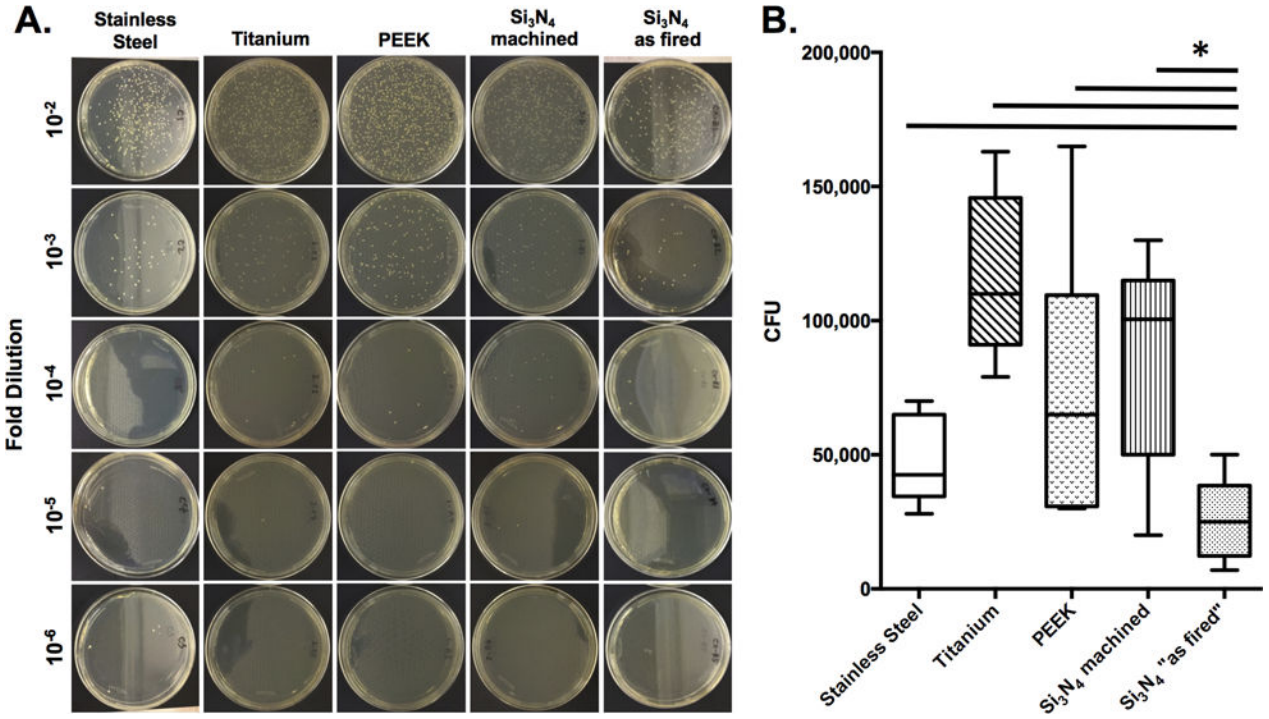

Figure 3. "As fired" Si_3N_4 implants display reduced colony forming units following exposure to MRSA in vitro

SS, Ti, PEEK and Si_3N_4 implants (n=4) were exposed to overnight cultures (O.D. = 0.7 at 630nm) of USA300 as described in Figure 1. After air drying, the implants were added to 1ml of sterile saline, vortexed, and serial dilutions were plated on tryptic soy agar (TSA) plates and incubated at 37°C for 24hrs to determine CFUs. Data from one of the equivocal replicate experiments is presented. Representative examples to illustrate the CFUs on the dilution plates are shown (A), and the CFU data are presented as the mean +/− SD (B; *p<0.002 1-way ANOVA).

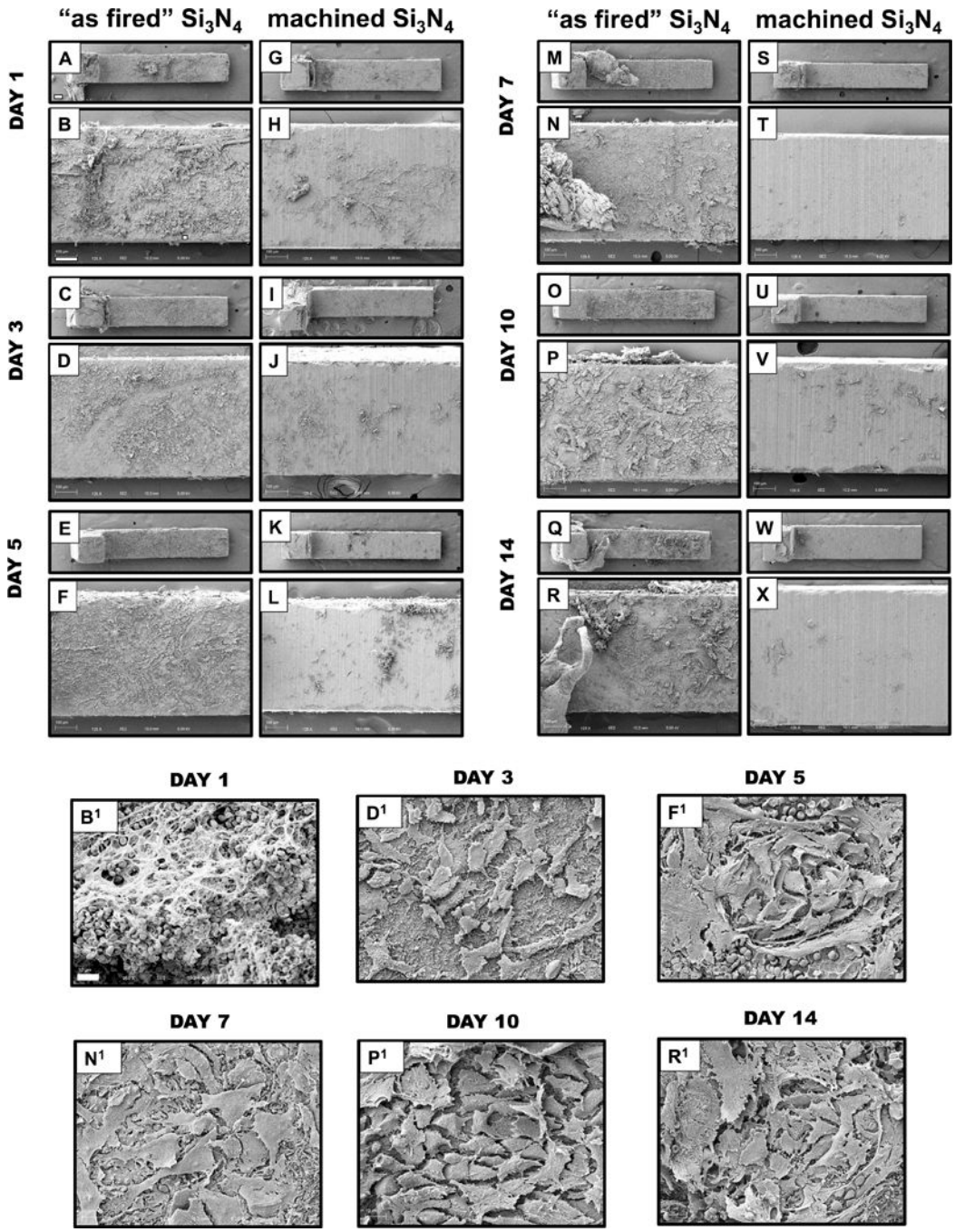

Figure 4. Differential host cell responses to sterile "as fired" vs. machined Si_3N_4 implants in bone over time

Sterile L-shaped "as fired" and machined Si_3N_4 implants (n=5) were surgically implanted into the tibiae of 6-week-old, female Balb/c mice, removed on the indicated day post-op, and processed for SEM (A-X). Representative low power images of the L-shaped implants are shown at × 30 (bar = 200μm), and higher power images of regions containing host material are shown at ×125 (bar =100μm). Of note is the highly reactive "as fired" Si_3N_4 implant surface, which displayed a progressive transformation towards osseous integration over time. Day 1 white and red blood cells (B, B^1×1000); Day 3 rounded/oval cells (mesenchymal stem

cells (MSCs)) (D, D^1×1000); Day 5 rounded to polygonal cells (differentiation MSCs) (F, F^1×1000); Day 7 Large polygonal mesenchymal cells (osteoblasts) (N, N^1 ×1000); Day 10 & Day 14 osteoblastic cells organizing to form a dense coating (P, P^1 ×1000 & R, R^1 ×1000, respectively). In contrast, machined Si_3N_4 implant surfaces were largely non-reactive with the host, and did not display any remarkable changes over time.

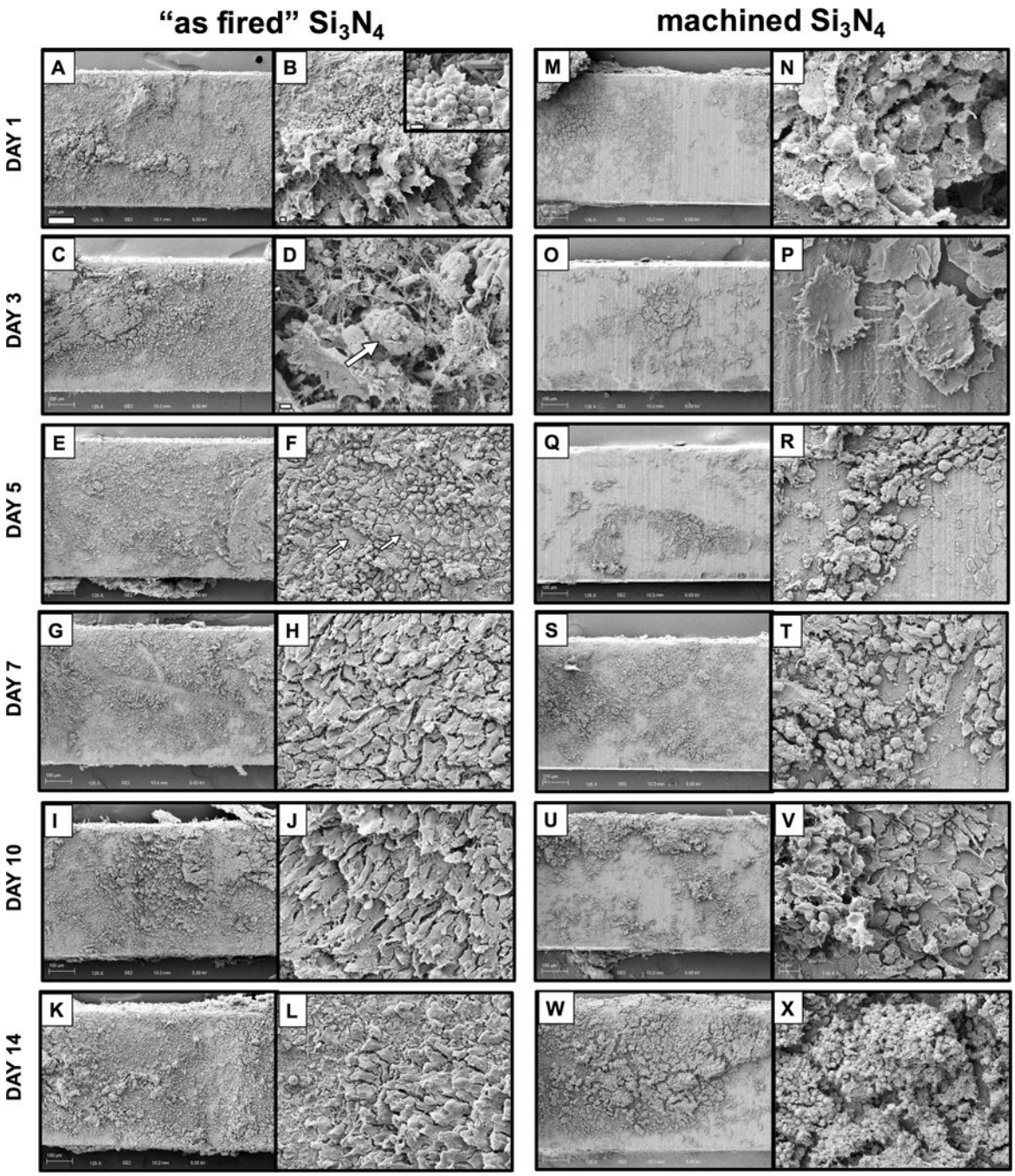

Figure 5. Differential host cell responses to MRSA contaminated "as fired" vs. machined Si_3N_4 implants in bone over time

Sterile L-shaped "as fired" and machined Si_3N_4 implants (n=3) were exposed to USA300LAC culture as described in Figure 1, surgically implanted into the tibiae of 6-week-old, female Balb/c mice, removed on the indicated day post-op, and processed for SEM (A-X). Representative ×125 images of the center of the L-shaped implants are shown (bar = 100μm), and higher power images of regions containing host material are shown at ×1,000 (bar =100μm). Of note is the highly reactive "as fired" Si_3N_4 implant surface, which displayed a progressive transformation from a MRSA infected surface, to and osseous

surface over time as follows. Day 1 bacterial biofilm (inset image ×5,000; bar = 1μm) is attacked by inflammatory cells (B; ×2,000 bar =2μm); Day 3 bacterial pod (arrow in D; ×5,000; bar = 1μm) is elevated from the surface by inflammatory cells anchored with fibrin cables; Day 5 eradicated bacteria are replaced by mixture of round cells (macrophages) and the appearance of a few polygonal cells (arrows in F; ×1,000; bar = 10μm); Days 7, 10 & 14 show polarized osteoblastic cells (H, J, L, ×1,000). In contrast, machined Si_3N_4 implant surfaces were less reactive with both bacteria and host cells as follows. Day 1 bacteria are rarely found in biofilm (N; ×5,000; bar = 1μm); Day 3 no bacteria are found, and few activated macrophages are present on the surface (P; ×3,000; bar = 2μm); Days 5, 7, 10 & 14 incomplete coating by red and white blood cells.